Permanent Magnet Synchronous Generators for Large Offshore Wind Farm Connected to Grid - Comparative Study between DC and AC Configurations

Djamel Ikni *‡, Morlaye Sekou Camara *, Mamadou Baïlo Camara *, Brayima Dakyo *, Hamid Gualous**

* Laboratoire GREAH - Université Le Havre, 75 rue Bellot, 76600 Le Havre –France

** Laboratoire LUSAC-Université de Caen, Rue Louis Aragon, 50100 Cherbourg -Octeville, France

(djamel.ikni@univ-lehavre.fr, brayima.dakyo@univ-lehavre.fr, camaram@univ-lehavre.fr, camarasekou2012@gmail.com, hamid.gualous@unicaen.fr)

‡ Corresponding Author; Djamel Ikni, 75 rue Bellot, 76600 Le Havre –France, Tel: + 3302 32 85 99 00
djamel.ikni@univ-lehavre.fr

Received: 06.05.2014 Accepted:04.06.2014

Abstract- This paper presents a comprehensive analysis of 10 MW large offshore wind farms ability to meet the requested energy imposed by electrical grid code by using DC and AC configurations. In DC configuration, the wind turbines are linked to DC-bus through the rectifiers, and all produced energy is injected in electrical grid via an inverter. In AC configuration, each wind turbine has a back to back converter for produced energy management, and the all subsystems are connected to grid through an AC-bus. The contribution of the paper presents two aspects: -The first aspect is focused on the energy management strategies using balance control, delta control and absolute control. -The second is related to the performances comparative study between the DC and AC configurations. For all configurations, the speed of the Permanent Magnet Synchronous Generator, the DC-bus voltage, and the exchanged power between wind farm and the network are controlled using grid code constraints (balance control, delta control and absolute control). To show the performances of the control strategies, some simulation results obtained with DC and AC configurations are presented and analyzed using Matlab/Simulink software.

Keywords Active and reactive power control; AC/DC converter; Grid code ; DC/AC converter; DC-bus voltage control; Offshore wind energy management; Permanent Magnet Synchronous Generator (PMSG); Speed control; Maximum Power Point Tracking (MPPT).

1. Introduction

In these last years, many researches are undertaken for the offshore wind farm system improvement, but the main challenges are focused on interconnection of the generators, and used converters for produced energy injection in the grid [1-4]. The DC and AC configurations are usually proposed in the literature, but the control strategies of these topologies presents some challenges.

This paper presents two contributions: -The first contribution is focused on the wind farm energy management using balance control, delta control and absolute control strategy. -The second contribution is based on the performances comparative study between DC and AC configurations. In DC configuration, the generators are linked to grid through the fully controlled frequency converters, which consist of two three phase rectifiers, an intermediate DC-bus, and a PWM inverter as illustrated in Fig.1. In AC configuration, each wind turbine has a back to back converter for produced energy management, and the subsystems are linked to electrical grid through an AC-bus as illustrated in Fig.2. The two configurations are connected to

AC grid of 20kV phase to phase RMS voltage. The proposed control strategies include the Maximum Power Point Tracking (MPPT) for PMSG speed control, the active/reactive power control, and DC-bus voltage control. To show the performances of the control strategies, some simulation results are presented and analyzed using Matlab/Simulink software. The obtained results in the normal operation (no fault in grid) from the DC configuration are compared to the AC configuration results.

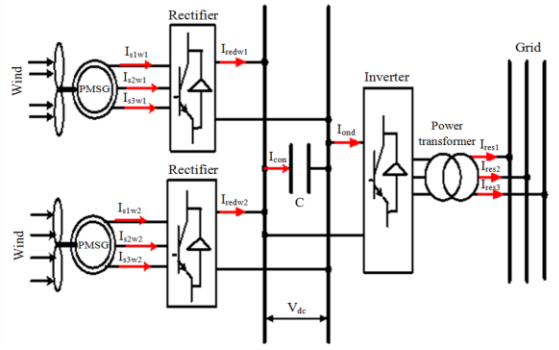

Fig.1. DC Configuration.

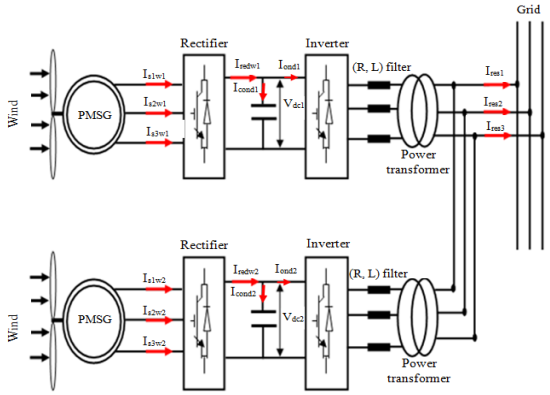

Fig.2. AC Configuration.

2. Wind energy conversion system modeling

2.1. Wind turbine modeling

The theoretical power generated by wind turbine is expressed in (1), where ρ is the density of the air; S is the circular area swept by the turbine; β is the angle of wedging of the blades, $V_{w1,w2}$ is the wind speed in [m/s].

$$P_{availw1,w2} = \frac{1}{2} \cdot C_p(\lambda,\beta) \cdot \rho \cdot S \cdot {V_{w1,w2}}^3, S = 2 \cdot \pi . R_t^2 \quad (1)$$

The ratio between the tip speed of the turbine and the wind speed is shown in (2), where Ω_m is the rotational speed of the turbine; R_t is the radius of the wind turbine.

$$\lambda = \frac{\Omega_m \cdot R_t}{V_{w1,w2}} \quad (2)$$

The C_p (λ, β) coefficient can be estimated using (3), and more information about this coefficient can be found in [5-6].

$$\begin{cases} C_p(\lambda,\beta) = 0.73.\left(\frac{151}{A} - 0.58.\beta - 0.02.\beta^{2.14} - 13.2\right).e^{\frac{18.4}{A}} \\ A = \frac{1}{\frac{1}{\lambda - 0.02.\beta} - \frac{0.003}{\beta^3 - 1}} \end{cases} \quad (3)$$

The torque of the wind turbine C_m obtained from the mechanical power is calculated using (4), where $P_{availw1,w2}$ is obtained from (1).

$$C_m = \frac{P_{availw1,w2}}{\Omega_m} \quad (4)$$

The mechanical equation of the system can be expressed as presented in (5), where J_t and J_m present respectively the inertia moments of the turbine and the generator; f_v is the coefficient due to the viscous rubbings of the generator; C_{em} presents the electromagnetic torque.

$$\begin{cases} (J_t + J_m).\frac{d\Omega_m}{dt} + f_v \cdot \Omega_m = C_m - C_{em} \\ J = J_t + J_m \end{cases} \quad (5)$$

2.2. PMSG modeling

PMSG dynamic model in the dq axis is expressed in (6); where R_s is the resistance in the stator; and L_d and L_q are the stator inductances; I_{sd} and I_{sq} present the currents in the stator; φ is the flux of the permanent magnet, p is the pair of poles [7].

$$\frac{d}{dt}\begin{bmatrix} I_{sd} \\ I_{sq} \end{bmatrix} = \begin{bmatrix} -\frac{R_s}{L_d} & \frac{p \cdot \Omega_m \cdot L_q}{L_d} \\ -\frac{p \cdot \Omega_m \cdot L_d}{L_q} & -\frac{R_s}{L_q} \end{bmatrix} \cdot \begin{bmatrix} I_{sd} \\ I_{sq} \end{bmatrix} + \begin{bmatrix} \frac{V_{sd}}{L_d} \\ \frac{V_{sq} - p \cdot \Omega_m \cdot \varphi}{L_q} \end{bmatrix} \quad (6)$$

In this paper, the smoothed poles permanent magnet synchronous generator is considered for system simulations which enables to write $L_d = L_q = L_s$.

2.3. AC/DC and DC/AC converters modeling

This section presents the average model of the converters (rectifier and inverter) obtained by considering the efficiencies of the converters are about 100%. Based on the Fig.1, the measured currents in the DC-bus can be expressed as presented in (7), where C is the DC-bus capacitor; I_{ond} is the inverter input current; $S_{a,b,c}$ present the three phase Pulse With Modulation (PWM) signals; $I_{s1w1,w2}$;$I_{s2w1,w2}$ and $I_{s3w1,w2}$ are the rectifiers input currents. The dynamic model of the rectifiers in AC configuration presented in Fig.2 can be deduced from (7) as illustrated in (8).

$$\begin{cases} I_{redw1} = S_a \cdot I_{s1w1} + S_b \cdot I_{s2w1} + S_c \cdot I_{s3w1} \\ C \cdot \frac{dV_{dc}}{dt} = I_{redw1} + I_{redw2} - I_{ond} \\ I_{redw2} = S_a \cdot I_{s1w2} + S_b \cdot I_{s2w2} + S_c \cdot I_{s3w2} \end{cases} \quad (7)$$

$$\begin{cases} C \cdot \dfrac{dV_{dc1}}{dt} = I_{redw1} - I_{ond1} \\ C \cdot \dfrac{dV_{dc2}}{dt} = I_{redw2} - I_{ond2} \end{cases} \quad (8)$$

The analytical model of the inverter is given in (9), where, V_{dc} is the DC-bus voltage, W_1, W_2 and W_3 present the PWM signals applied to inverter. To obtain the model of the inverters in AC configuration, V_{dc} must be replaced respectively by V_{dc1} and V_{dc2}.

$$\begin{cases} V_{Sa} = \dfrac{2 \cdot W_1 - W_2 - W_3}{3} \cdot V_{dc} \\ V_{Sb} = \dfrac{2 \cdot W_2 - W_1 - W_3}{3} \cdot V_{dc} \\ V_{Sc} = \dfrac{2 \cdot W_3 - W_1 - W_2}{3} \cdot V_{dc} \end{cases} \quad (9)$$

2.4. Electrical grid modeling

To establish the model of electrical grid presented in Fig.3, balanced three phase system is considered. The V_{res1}, V_{res2} and V_{res3} voltages are connected to inverter through a transformer with ratio of *m*. Based on Fig.3; the analytical model of the grid is presented in (10), where e_1, e_2 and e_3 present the conventional three phase *emf* of the grid with phase to phase *RMS* voltage of 20kV.

$$\begin{cases} V_{res1} - e_1 = R_{res} \cdot I_{res1} + L_{res} \cdot \dfrac{d}{dt}(I_{res1}) \\ V_{res2} - e_2 = R_{res} \cdot I_{res2} + L_{res} \cdot \dfrac{d}{dt}(I_{res2}) \\ V_{res3} - e_3 = R_{res} \cdot I_{res3} + L_{res} \cdot \dfrac{d}{dt}(I_{res3}) \end{cases} \quad (10)$$

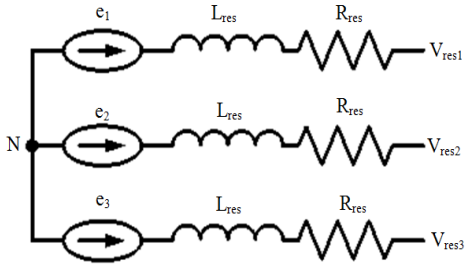

Fig.3. Electrical grid model.

3. DC configuration control strategy

The proposed control strategies include: - PMSG speed control based on Maximum Power Point Tracking (MPPT) technique. - Active and reactive powers control using the inverter connected to grid. - DC-bus voltage control through the rectifiers connected to stator. The similar control strategies are presented in [8] for wind turbine application based on the doubly feed induction generator.

3.1. PMSG speed control strategy

Speed references for the two wind turbines are expressed in (11), where $v_{w1,w2}$ present the wind speed profiles for two wind turbines. These references are obtained from MPPT technique. The control strategy of the two PMSG speeds is illustrated in Fig.4.

$$\Omega_{refw1,w2} = \frac{\lambda_{opt} \cdot v_{w1,w2}}{R_t} \quad (11)$$

The PI controller coefficients obtained from closed loop analysis are shown in (12), where ω_{nd} presents the dynamics of the system, and t_{sd} is the control loop time constant, [9].

$$\begin{cases} K_p = \sqrt{2} \cdot \omega_{nd} \cdot (J_t + J_m), \omega_{nd} = \dfrac{5.8}{t_{sd}} \\ K_i = \omega_{nd}^2 \cdot (J_t + J_m) \end{cases} \quad (12)$$

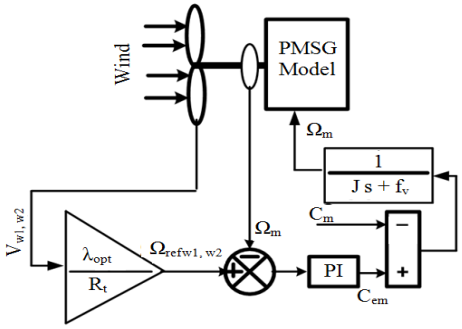

Fig.4. PMSG speed control loop for each wind turbine.

3.2. Active and reactive power control

The active and reactive powers injected in electrical grid is estimated using (13), where (V_{dres},V_{qres}) and (I_{dres},I_{qres}) are respectively the grid voltage, and the injected current in the grid.

$$\begin{cases} P_{wf} = V_{dres} \cdot I_{dres} + V_{qres} \cdot I_{qres} \\ Q_{wf} = V_{qres} \cdot I_{dres} - V_{dres} \cdot I_{qres} \end{cases} \quad (13)$$

To simplifying the control strategy, the majority of the authors choose a reference frame related to the stator. However, this choice is not best in this application, because the parameters which must be controlled are in the stator side (P_{wf}, Q_{wf}). The choice of an axes system shifted 90° behind on the vector of grid voltage (V_{dres} = *0* and V_{qres} = V_{res}) is much more advantageous [10]. Based on this assumption, the approximate active and reactive power injected in electrical grid can be expressed as presented in (14). This equation shows that, the active power can be controlled through I_{qres} current, and the reactive power can be controlled using I_{dres}.

$$\begin{cases} P_{wf} \approx V_{res} \cdot I_{qres} \\ Q_{wf} \approx V_{res} \cdot I_{dres} \end{cases} \quad (14)$$

The active and reactive power control strategies are presented in Fig.5, where PI is the Proportional Integral controllers. The coefficients of the PI controllers used in the inner and the outer loops are respectively presented in (15).

$$\begin{cases} K_{pir} = \dfrac{2.197 \cdot L_{res}}{t_{ir}} \\ K_{iir} = \dfrac{2.197 \cdot R_{res}}{t_{ir}} \end{cases}; \begin{cases} K_{pp} = \dfrac{t_{ir}}{t_p} \\ K_{ip} = 2.197 \cdot t_p \end{cases} \quad (15)$$

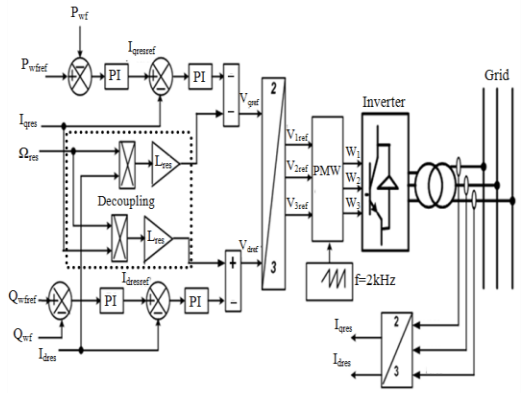

Fig.5. Active and reactive power control loops.

3.3. DC-bus voltage control method

The control strategy of the DC-bus voltage is presented in Fig.6, where the reference current I_{qref} is obtained from the DC-bus voltage control loop. I_{dref} is fixed to zero to obtain a power factor equal to 1. Like to PMSG speed control, the PI controller is used for the DC-bus voltage management. The coefficients of this controller are shown in (16), where ω_n is the dynamics of the system, and t_{sdc} is the DC-bus voltage control loop time constant.

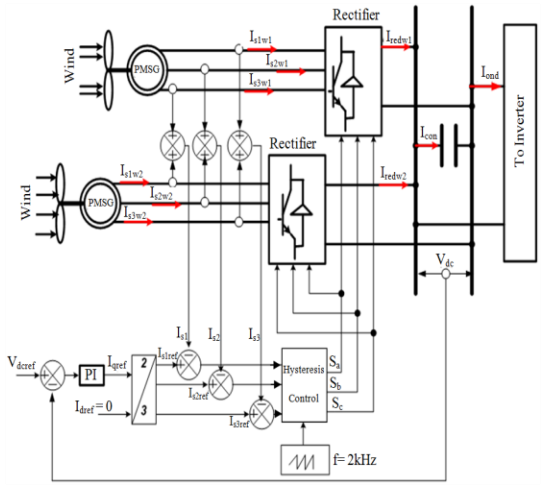

Fig.6. DC-bus voltage control strategy.

$$\begin{cases} K_{pdc} = \sqrt{2} \cdot \omega_n \cdot C \\ K_{idc} = \omega_n^2 \cdot C \end{cases}, \quad \omega_n = \frac{5.8}{t_{sdc}} \qquad (16)$$

4. AC configuration control strategy

The AC configuration presented in Fig.2 includes, two wind turbines based on PMSG with rated power of 5MW for each generator; two back to back converters and two transformers. The converter in PMSG side is used to control the torque and the generator's speed for each wind turbine. Used converter in electrical grid side for each wind turbine ensures the DC-bus control, the active and reactive power management between generator and grid. These converters provide a complete decoupling between the electrical grid and generators. More information about this method can be found in [11] and [13]. The control strategy for each generator includes three subsystems. First is based on the vector control of the PMSG also called Field Oriented Control (FOC), the second is the Maximum Power Point Tracking (MPPT), and the last is the pitch control [11-14].

4.1. Stator's current control method

The vector control strategy applied in this study consists to impose a reference for *d*-axis current I_{sd} equal to zero as presented in Fig.7. More information about this method can be found in [12] and [13]. The control of the electromagnetic torque is based on I_{sq} current as illustrated in (17).

$$C_{em} = \frac{3}{2} \cdot p \cdot \varphi \cdot I_{sq} \qquad (17)$$

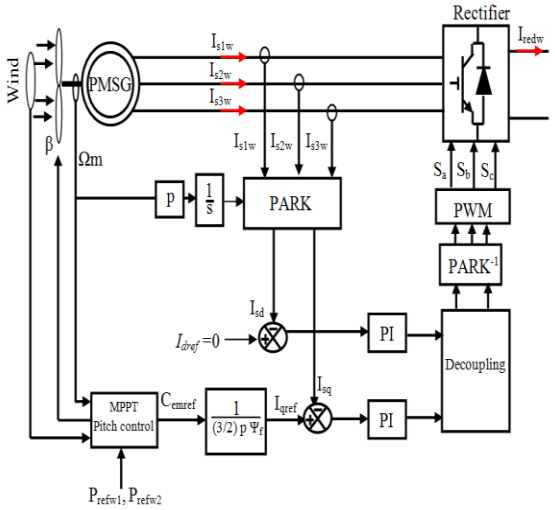

Fig.7. Stator's currents control loops.

4.2. Maximum power point tracking (MPPT) and pitch angle control method

The PMSG speed control is based on MPPT and it is same to that presented in Fig.8 shows that, in the each wind speed there is an optimal speed of the turbine which corresponds to the maximum power. A pitch angle control is used to reduce the aerodynamic power captured by the wind, and to keep the output power of PMSG at the power reference when the wind speed is greater than the nominal speed [11]. The control method of the pitch angle is shown in Fig.9.

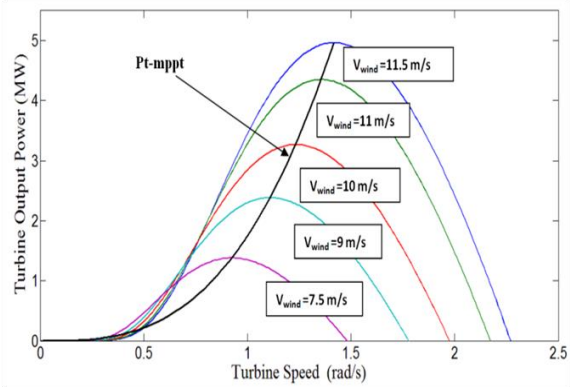

Fig.8. Principle of the MPPT.

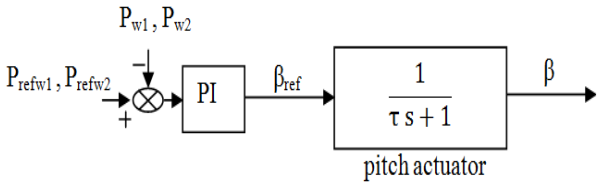

Fig.9. Pitch angle control method.

4.3. DC-bus voltage and reactive power control strategies

Grid side converter control includes the inner loops based on the grid currents management, and two outer loops focused on DC-bus voltage and reactive power management as shown in Fig.10. The similar methods are presented in [12], and [15-19]. The parameters of the PI controllers are estimated using (15), and (16).

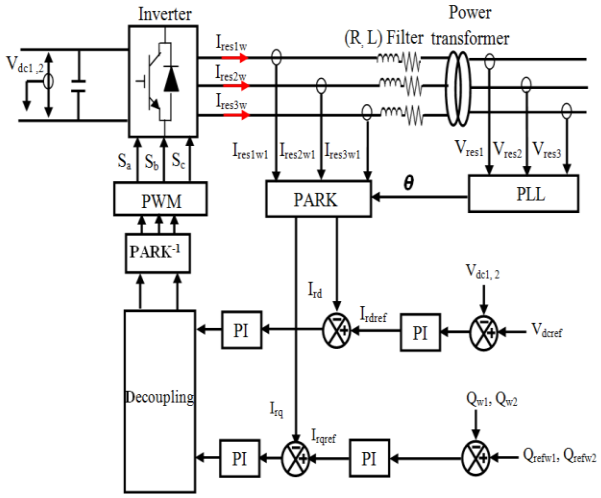

Fig.10. DC-bus voltage and reactive power control strategies.

5. Power references estimation using grid code constraints

The wind farm controller is the "brain center" of the wind farm. Its role is to control the total power that is required and authorized to inject in electrical grid by the wind farm. The overall objective of such a controller is to allow the wind farm to behave as active element, and to participate to grid services. To do this operation, the balance control, the delta control and absolute control are necessary.

5.1. Principle of balance ,delta and absolute control

The balance control principle is presented in Fig.11a, where P_{wfref} presents the active power demanded by grid operator, and $P_{wfavail}$ is available power from generators. In this mode, the wind farm has to be capable of increasing or decreasing rapidly its power to a given fixed value. This feature has its utility if the grid operators would have to act fast to maintain the balance between production and consumption.

Delta control principle is illustrated in Fig.11b. In this case, the produced power (energy) must be limited to a percentage of the available power (85% in this paper). So, the wind turbine can contribute in the primary regulation of the frequency.

Figure.11c shows the absolute control principle. For this type of control, the injected power in electrical grid by the wind farm is limited to a maximum defined by the network manager. Below this power, wind turbines can operate normally, [20-21].

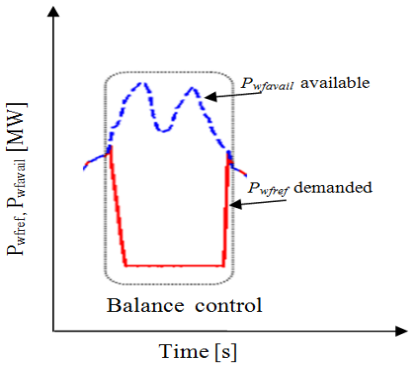

Fig.11a Balance control principle.

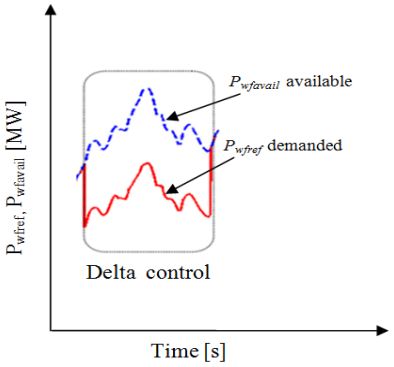

Fig.11b Delta control principle.

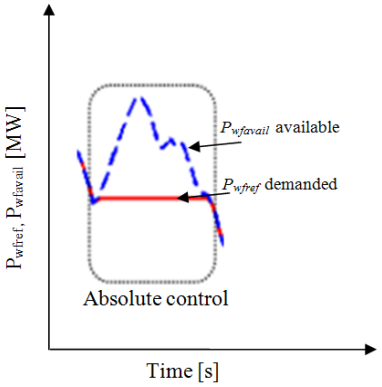

Fig.11. Absolute control principle.

5.2. Active and reactive power references estimation using grid code constraints

Figure.12 presents the references estimation of the active and reactive power for the wind farm [20]. The control unit presented in Fig.12 necessitate in its input: - the requirements of the system operator (balance control, delta control and the absolute control); - the measured powers in the point of common coupling; - and available power in wind farm, [20-21]. In this paper, it is considered that, the electrical grid is in

normal operation (not fault in electrical grid). This assumption enables to use Fig.12 without the control of the frequency f_{pcc} and the voltage V_{pcc} in point of coupling to grid. In dispatch control block presented in Fig.12, the active and the reactive power references for each wind turbine is calculated using a proportional distribution algorithm method as presented in (18), where $P_{availw1,2}$ and $Q_{availw1,2}$ present the available active and reactive powers for each wind turbine. More information about this method can be found in [20] and [21]. The active and reactive powers available in the wind farm are calculated using (19), where $tan(\Phi)=0.327$ corresponds to electrical power factor.

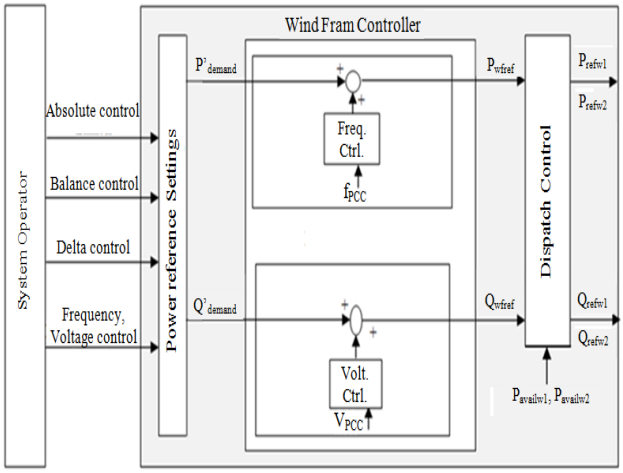

Fig.12. Active and reactive power references estimation.

$$\begin{cases} P_{refw1} = P_{wfref} \cdot \dfrac{P_{availw1}(C_{p\max})}{P_{availw1}(C_{p\max}) + P_{availw2}(C_{p\max})} \\ Q_{wfref} = \tan(\Phi) \cdot P_{wfref} \\ Q_{refw1} = Q_{wfref} \cdot \dfrac{Q_{availw1}}{Q_{availw1} + Q_{availw2}} \\ P_{refw2} = P_{wfref} \cdot \dfrac{P_{availw2}(C_{p\max})}{P_{availw1}(C_{p\max}) + P_{availw2}(C_{p\max})} \\ Q_{refw2} = Q_{wfref} \cdot \dfrac{Q_{availw2}}{Q_{availw1} + Q_{availw2}} \end{cases} \quad (18)$$

$$\begin{cases} P_{wfavail} = P_{availw1}(C_{p\max}) + P_{availw2}(C_{p\max}) \\ Q_{wfavail} = Q_{availw1} + Q_{availw2} \\ Q_{availw1} = \tan(\Phi) \cdot P_{availw1}(C_{p\max}) \\ Q_{availw2} = \tan(\Phi) \cdot P_{availw2}(C_{p\max}) \end{cases} \quad (19)$$

For DC configuration, the active and reactive power references are estimated using (20).

$$\begin{cases} P_{wfref} = P_{refw1} + P_{refw2} \\ Q_{wfref} = P_{wfref} \cdot \tan(\Phi) = 0.327 \cdot P_{wfref} \end{cases} \quad (20)$$

6. DC and AC configuration simulation results

6.1. *DC configuration simulation results*

For system simulations, the wind turbines references speeds are estimated using (11). The references of the active and reactive powers are estimated using (20). DC-bus voltage reference is respectively fixed to 5kV and 5.5kV to show the performances of the control. By convention, the sign of the reactive power is assumed positive for the supplied power, and negative for consumed power. Used parameters for system simulations are presented in Appendix section.

Figure.13 shows the wind speed profiles for two wind turbines, where the minimum and maximum values are respectively to 8.5m/s and 11.5m/s with an average value of 10.5m/s. The speeds control results of the wind turbines are presented in Fig.14 and Fig.15. These curves show that, the proposed control strategy is satisfactory, i.e. measured speeds are close to the references.

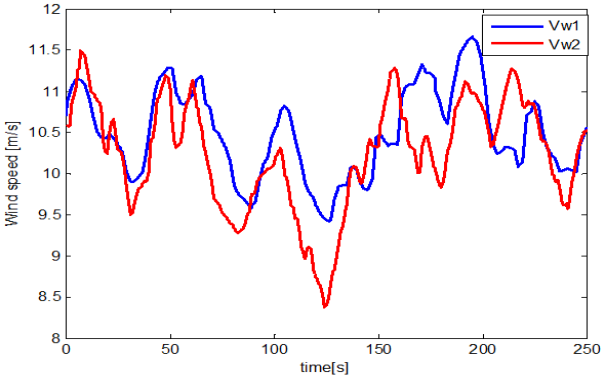

Fig.13. Wind speed profiles for two wind turbines.

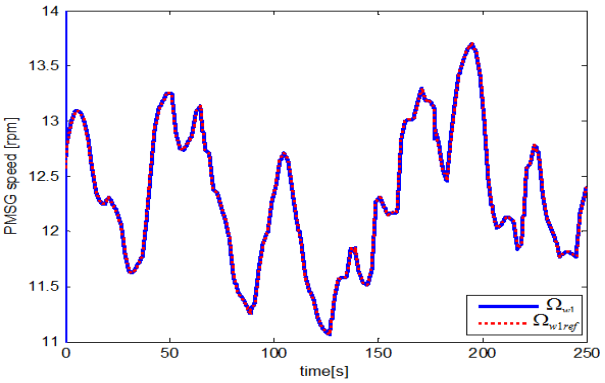

Fig.14. PMSG Speed control result for first wind turbine without pitch angle control.

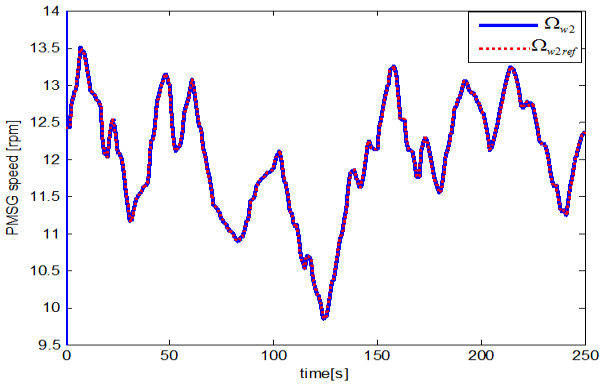

Fig.15. PMSG Speed control result for second wind turbine without pitch angle control.

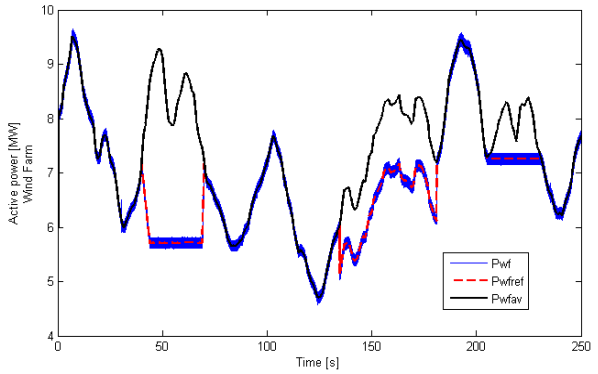

Fig.16. Active power control result obtained with balance, delta and absolute controls.

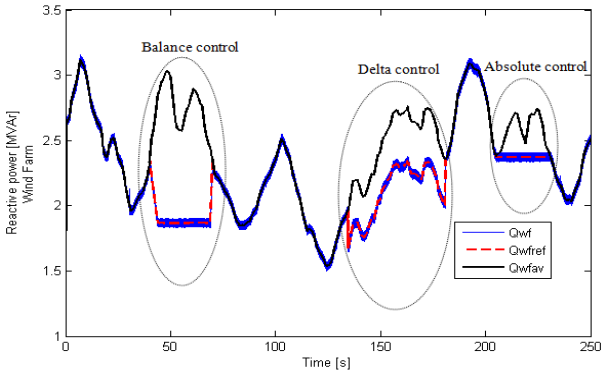

Fig.17. Reactive power control result obtained with balance, delta and absolute controls.

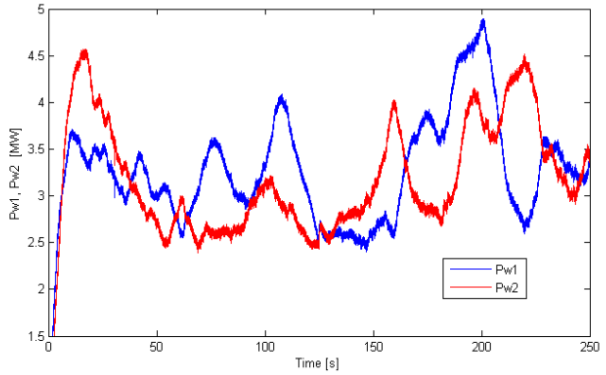

Fig.18. Contribution of each wind turbine obtained with balance, delta and absolute controls.

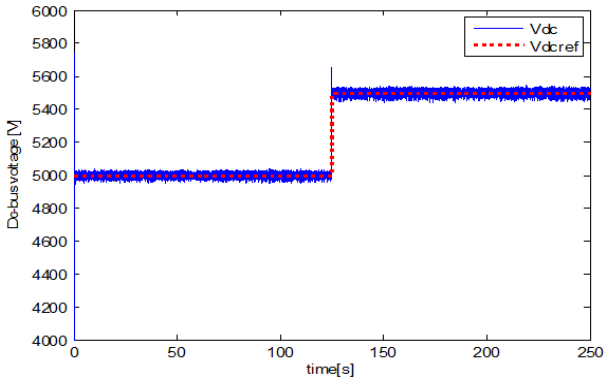

Fig.19. DC-bus voltage control result.

The active and reactive powers control results are respectively presented in Fig.16 and Fig.17. These results allow to concluding the control strategies presented in Fig.5 are adequate. Measured powers compared to the references show that the control strategies take into account the wind speeds variations. Figure.18 presents the contribution of each wind turbine in the DC-bus, where P_{w1} and P_{w2} are not the same due to wind speeds behaviors. The DC-bus voltage control result is plotted in Fig.19. This figure shows that, the measured voltage follows the reference ones, which enables to conclude that the proposed control is performing.

6.2. AC configuration simulation results

Wind turbines are controlled to extract the maximum power if the wind speed is less than its maximal value (11.5m/s). PMSG speeds control results obtained from MPPT method are plotted in Fig.20 and Fig.21. To limit the produced energy from the wind turbines and to meet the power profile imposed by the grid operator a pitch angle control is used. The pitch angle control action is illustrated in Fig.20 and Fig.21, precisely from 40 to 70s, 134 to 181s, and 205 to 231s. These intervals of the time coincide respectively to the balance control, delta control, and absolute control. Figure.22 shows the total active power injected in electrical grid obtained with the balance, the delta and the absolute controls. The reactive power injected in the grid follows perfectly the dynamic variations of the reference as presented in Fig.23. Figure.24 presents the active power for each wind turbine, where the variations of P_{w1} and P_{w2} are due to intermittent behavior of the wind speed. Figure.25 shows the DC-bus voltage control result where V_{dc1} is same to V_{dc2}.

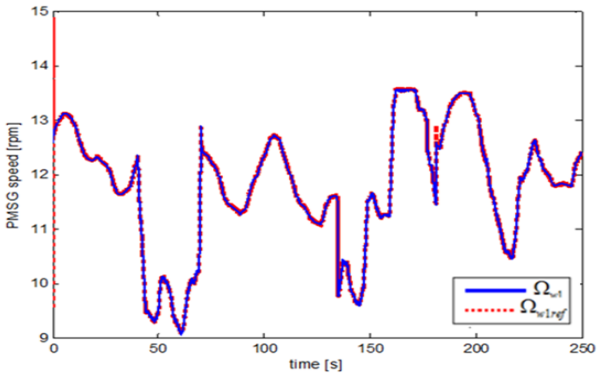

Fig.20. PMSG Speed control result for first wind turbine with pitch angle control.

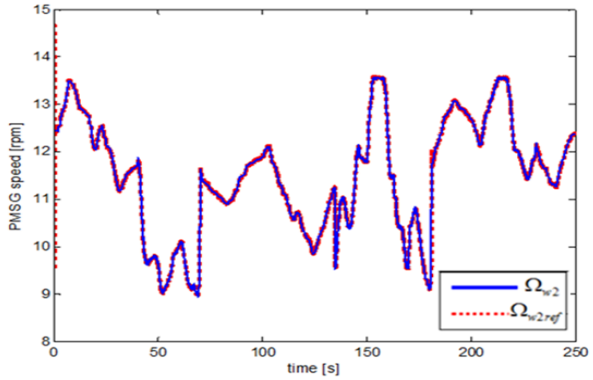

Fig.21. PMSG Speed control result for second wind turbine with pitch angle control.

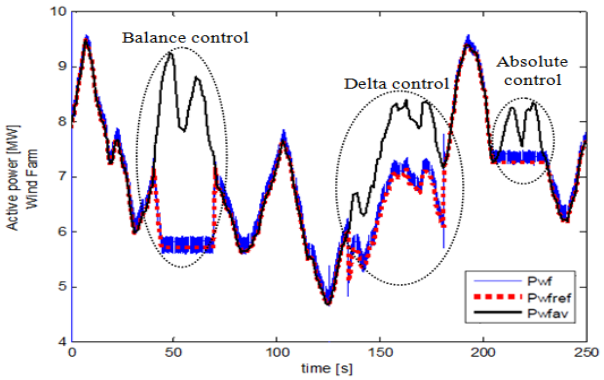

Fig.22. Active power control result obtained with the balance, the delta and the absolute controls.

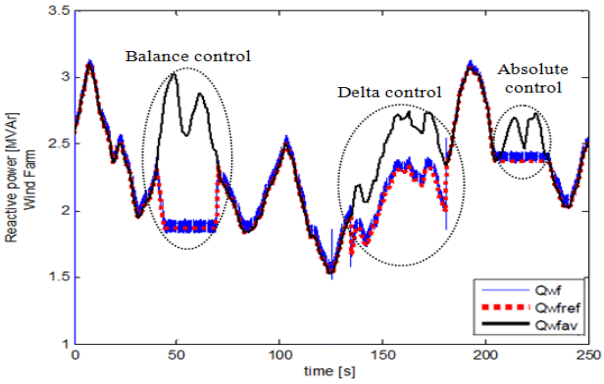

Fig.23. Reactive power control result obtained with the balance, the delta and the absolute controls.

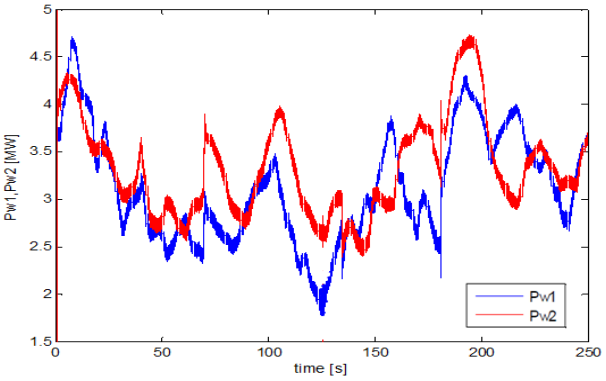

Fig.24 Contribution of each wind turbine in the DC-bus.

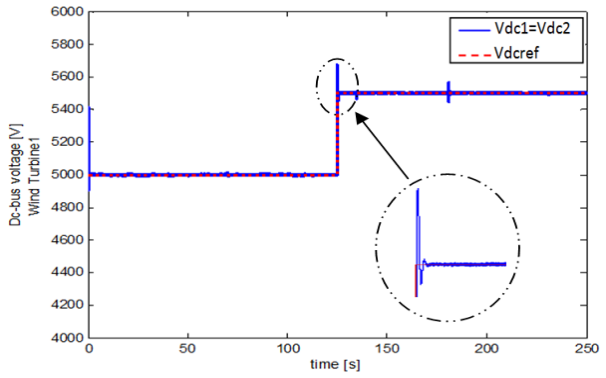

Fig.25. DC-bus voltage control result for the first and the second wind turbine.

These curves are identical to reference voltage except during the sudden variation of the reference, where the DC-bus voltage control loops have not enough time to react.

7. Conclusion

In this paper, the authors present the modeling and control of the wind farm based on the Permanent Magnet Synchronous Generators connected to AC grid through the back-to-back converters. Two configurations of the offshore wind farm are studied and analyzed. The first configuration is based on DC configuration, and the second is focused on AC configuration. The proposed control strategies (balance control, delta control and the absolute control) allow to the wind farm to behave as active element, and to participate to grid services. Based on simulation results, the performances of the two configurations are same but the DC-configuration needs less components (converter and transformer) compared to AC configuration. In more, the control strategy is easy to implement compared to AC configuration. Finally, the DC configuration seems to be interesting compared to that of the AC configuration for offshore wind energy applications without the consideration of the safety problems.

8. Appendix

P_n	PMSG rated power	5 MW
R_t	Radius of the wind turbine	56 m
ρ	Air density	1.22 kg/m
R_s	Resistance of PMSG	6.25mΩ
L_s	Inductance of the PMSG	4.2 mH
J	Inertia of wind turbine	10^4 kg.m^2
p	Pair of poles	75
U_{sef}	RMS voltage in the stator	690V
V_{dcref}	DC-bus voltage reference	5kV to 5.5kV
R_{res}; L_{res}	Electrical grid parameters	50 Ω; 0.7H
R; L	Parameters of the filter	0.5mΩ; 0.3mH
C	DC-bus capacitor	5mF
φ	Magnetic induced flux	11Wb
τ	Pitch actuator time constant	0.7s
P_{wfref}	Active power demanded by grid operator	
$P_{wfavail}$	Available power from generators	
$P_{availw1}$, $P_{availw2}$	Available active power from each wind turbine	
$Q_{availw1}$, $Q_{availw2}$	Available reactive power from each wind turbine	
C_{pmax}	Maximum power coefficient for wind turbines	0.53
λ_{opt}	Optimal ratio between speed of the turbine and wind speed	6.89

References

[1] Fujin Deng "Design and control of A DC grid for offshore wind farms "Ph.D. dissertation. The Faculty of Engineering, Science, and Medicine, Univ. Aalborg, Denmark, 2012

[2] P. Bresesti, Wil L. Kling, Ralph L. Hendriks, and R. Vailati"HVDC connection of offshore wind farms to the transmission system" IEEE Transaction on energy conversion, vol.22, no.1, pp.37-43, March 2007.

[3] L. Max, "Design and control of a DC collection grid for a wind farm"Ph.D.dissertation .Dept of Energy and Environment, Univ. Goteborg, Sweden, 2009.

[4] S.Lundberg "Conguration study of large wind parks" Ph.D. dissertation .Deptof Energy and Environment, Univ. G¨oteborg, Sweden, 2003

[5] F. D. Bianchi, H. D. Battista, and R. J. Mantz, "Wind Turbine Control Systems: Principles, Modelling and Gain Scheduling Design", London Springer, 2007.

[6] B. Singh and S. Sharmay, "Stand-alone wind energy conversion system with an asynchronous generator", Journal of Power Electronics, vol. 10, no. 5, pp. 538-547. Sept. 2010.

[7] A.E. Fitzgerald, C. Kingsley, Jr., and S.D. Umans; "Electric Machinery", Textbook Sixth Edition. New York: McGraw-Hill, 2003.

[8] M.S.Camara; M.B. Camara; B.Dakyo; H.Gualous, "Modeling and Control of the Offshore wind energy system based on 5MW DFIG connected to grid'', IEEE-AFRICON Conference, pp.991-995;2013.

[9] A. Tapia, G. Tapia, and J. Ostolaza, "Modeling and control of a wind turbine driven doubly fed induction generator," IEEE Trans. Energy Conversion, vol. 18, no. 2, pp. 194–204, 2003.

[10] T. Senjyu, R. Sakamoto, and N. Urasaki, "Output power leveling of wind turbine generator for all operating regions by pitch angle control", IEEE Trans. Energy Conversion, vol. 21, no. 2, pp. 467–475, 2006.

[11] Guangchen Liu, Shengtie Wang, Hong Zhang, and Bo Wang, "Integrated Control Strategy of Multibrid Wind Power Generation System", IEEE 7th Inter. Power Electronics and Motion Control Conf. - ECCE Asia. June 2-5, 2012, Harbin, China.

[12] D.Ikni, M.B. Camara, A.Payman and B.Dakyo "Dynamic control of wind energy conversion system", Inter. conference and exhibition on Ecological Vehicles and Renewable Energies (EVER'13) to be held at Monaco/France on March 27-30, 2013.

[13] Lijun He , Yongdong Li , and Ronald G. Harley "Adaptive Multi-mode Power Control of a Direct-Drive PM Wind Generation System in a Micro grid", IEEE journal of emerging and selected topics in power electronics , Vol.1, no. 4, pp. 217-225. Dec 2013.

[14] Mandic, G. ; Nasiri, A. ; Ghotbi, E. ; Muljadi, E., "Lithium-Ion Capacitor Energy Storage Integrated With Variable Speed Wind Turbines for Power Smoothing", IEEE Journal of emerging and selected topics in power electronics, vol. 1, no. 4, Dec.2013.

[15] Mohamed Mansour, M. N. Mansouri, M.F. Mmimouni, "Study and Control of a Variable-Speed Wind-Energy System Connected to the Grid", Inter. Jour. of Renewable Energy Research, IJRER, Vol.1, No.2, pp.96-104, 2011.

[16] Junbiao Han, Sarika Khushalani Solanki,and Jignesh Solanki," Coordinated Predictive Control of a Wind/Battery Microgrid System", IEEE Journal of emerging and selected topics in power electronics, vol. 1, no. 4, Dec. 2013.

[17] V. Yaramasu; B. Wu, "Predictive Control of Three-Level Boost Converter and NPC Inverter for High Power PMSG-Based Medium Voltage Wind Energy Conversion Systems", IEEE Trans. on Power Electro., Vol. PP, no: 99, 2013.

[18] M.O.F.Diallo, M.B. Camara , S. Youssef, H.Gualous, B. Dakyo, "Energetic capability Characterization of the Raz Blanchard area for the tidal turbine farm implementation", IEEE Inter. Conf., AFRICON, 9- 12 Sept.2013, Mauritius.

[19] M.B. Camara, B. Dakyo, C. Nichita, G.Barakat, "Simulation of a Doubly Fed Induction Generator with Hydro Turbine for Electrical Energy Production", IEEE Inter. Conf. Electromotion 2009, July 1-3, Lille, FRANCE, Proceedings CD.

[20] D.Ikni, B.Dakyo, A.O.Bagre, " Large Offshore Wind Farm: Potential Evaluation of Network Services ", PowerTech 2013, IEEE Conference, 16-20 juin 2013, Grenoble, France.

[21] Cosmin E. Bănceanu, Iulian V, " Coordinated control of wind turbine" , Master Thesis, Dept. Energy Technology - Pontoppidanstræde 101 Aalborg , Univ Aalborg , Denmark, 2011.